Supplementary Material

S1. Sample fabrication process

The MESA of the device, with dimensions 250×650 μm^2, was prepared in GaAs/AlGaAs heterostructure by wet etching in H_2O_2: H_3PO_4: H_2O =1:1:50 for 100 seconds. The 2DEG was located 170 nm below the surface. Ohmic contacts were deposited at the edge of the MESA and within the MESA area (for testing the interface modes). The sequence of the evaporation by order was: Ni (15 nm), Au (260 nm), Ge (130 nm), Ni (87.5 nm), Au (15 nm). Contacts were annealed at 440℃ for 80 seconds. The sample was covered by 30nm of an insulating HfO_2 followed by evaporation of large metal gates, Ti (5 nm) and Au (15 nm). The latter separated the device area into three regions with fillings: ν_a, ν_b, ν_d. In the following step, the MESA was covered by 25 nm of HfO_2 layer, followed by a deposition of quantum point contacts (QPCs), a modulation gate (MG), and a small top gate (TG) in the middle of the bulk, with diameter 0.5 μm and or 0.35 μm. In the final step, ohmic contacts, large metallic gates, the QPCs, and the modulation gate (MG) were connected to large pads via thick gold lines. The TG was connected by an *air bridge* and gold lines that passed over the HfO_2-coated metallic gates.

S2. Interfacing hole-conjugate states

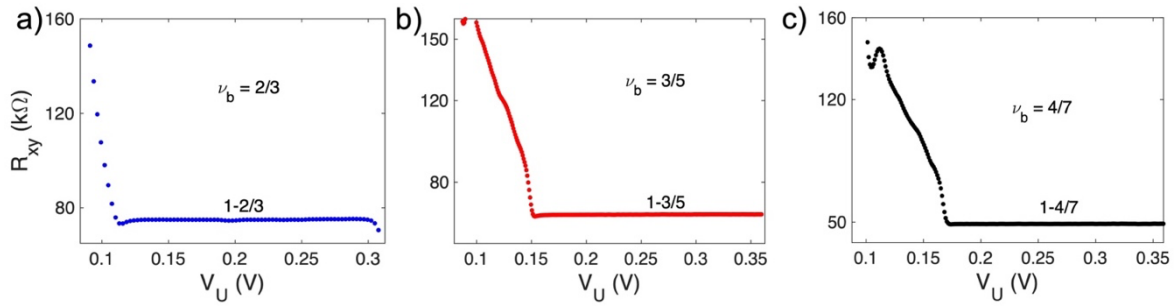

Figure S2. Interfacing hole-conjugate states. Two-terminal resistance measurements of the interface between ν_b and ν_a. The bulk filling factor is fixed at ν_b= 2/3 **(a)**, 3/5 **(b)**, and 4/7 **(c)**, while the accumulation gate is swept on the conductance plateau of ν_a=1, with a positive bias. At ν_b=2/3 and ν_a=1, the 2DEG density underneath the gate increases by ~50%. Once charge equilibration is achieved, all interface modes move in the downstream direction.

S3. Dependence of flux periodicity on the interface modes

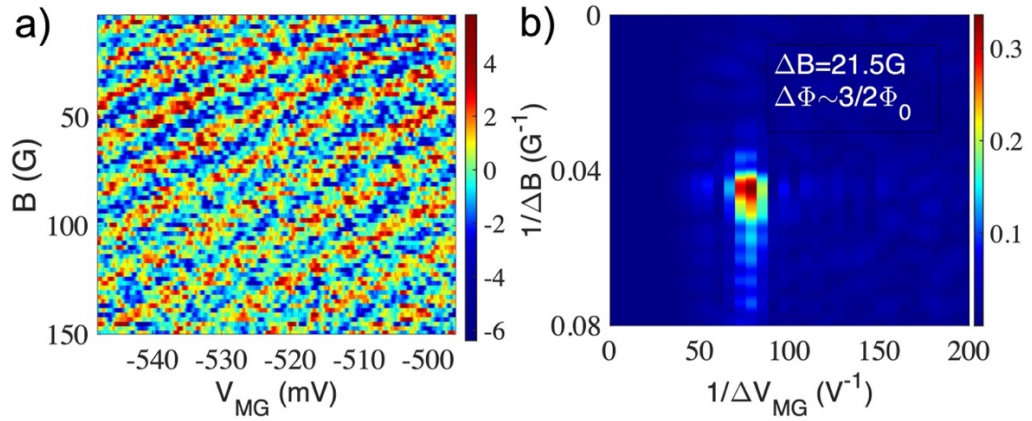

Figure S3. Aharonov-Bohm interference configuration ν_a=4/3, ν_b=2/3, ν_d=0. (a) Conductance oscillations for ν_b=2/3 in the B-V_{MG} plane, with 2DEG density underneath the accumulation gate is increased by ~100%. The top gate in the bulk is not charged (V_{TG}=0V). **(b)** The 2D FFT of the pajama plot shows a single peak with the periodicity ΔB=21.5 G, ΔV_{MG}=12.7mV. The flux periodicity is $\Delta\Phi \approx (3/2)\Phi_0$, for an AB area of ~3μm². Similar results were observed in the fillings combination '1-2/3-0' (see main text) and '1-2/3-1/3', suggesting that the bulk filling solely determines the flux periodicity. Although the configuration of the upstream neutral mode is different in the configuration 4/3-2/3-0 (downstream neutral at '4/3-2/3' and upstream neutral at '2/3-0') and in 1-2/3-0 (one upstream neutral mode at the '2/3-0' interface) and 1-2/3-1/3 (two upstream neutral at '2/3-1/3' interface), all suggesting that the fractional flux periodicity is not affected by the nature of the edge modes.

S4. The effect of positive top gate potential on the bunched anyons

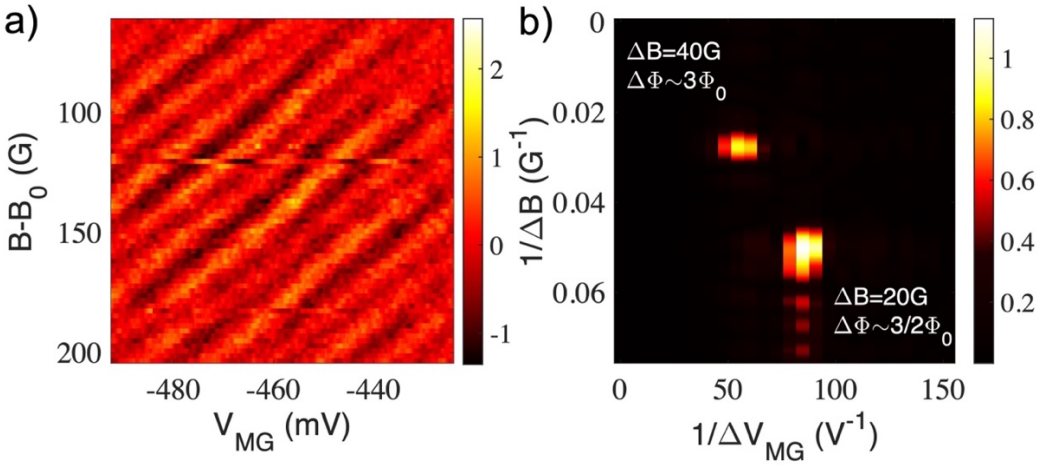

Figure S4. Dissociation of bunched anyons via charging the TG: (a) AB pajama with $\nu_b = 2/3$, and filling factors configuration: '1-2/3-0'. The QPCs are biased for transmission of 80% and top gate voltage is V_{TG}=+0.03V. **(b)** 2D FFT with two distinct peaks: The most prominent peak with flux periodicity $\Delta\Phi \sim (3/2)\Phi_0$ corresponds to the interference of a 'bunched' QP with charge 2e/3. The weaker peak with flux periodicity $\boldsymbol{\Delta\Phi \sim 3\Phi_0}$ corresponds to the interference of elementary QPs with a charge e/3, suggesting partial dissociation of the bunched QPs. Note that the modulation gate voltage periodicity (ΔV_{MG}) is almost twice as large in the dissociated condition. For a negative TG potential, see the main text.

S5. Analysis of the deconvoluted peaks using the Gaussian filtering method

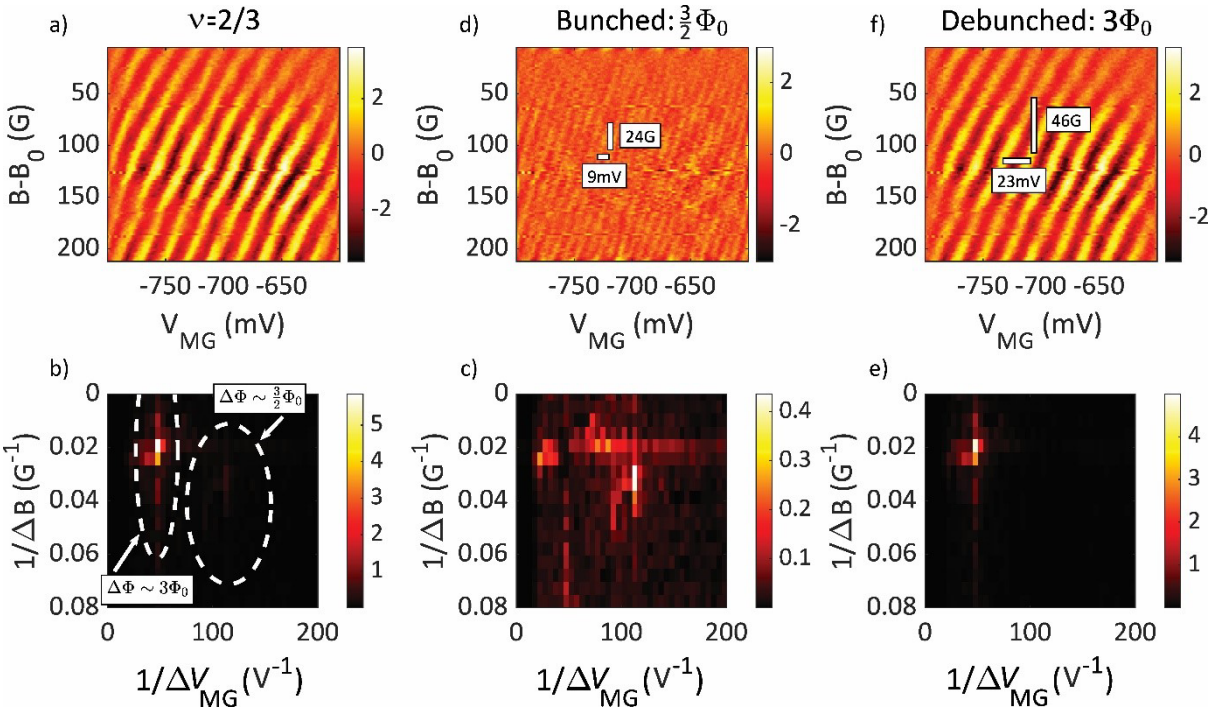

Figure S5a. Separate views of flux periodicities at filling ν=2/3 with charged top gate. (a) A strong peak at $\Delta\Phi=3\Phi_0$ (dissociated QPs) and a residual peak at $\Delta\Phi\cong(3/2)\Phi_0$ (bunched QPs) **(b)** Two corresponding peaks in the FFT. The dotted ovals indicate the radius of the Gaussian filtering applied later. **(c)** Removing the dissociated FFT peak at $3\Phi_0$ by Gaussian filtering and leaving the weaker peak of the bunched QPs. **(d)** Returning to *real space* pajama of the bunched QPs, with periodicity $\Delta\Phi\cong(3/2)\Phi_0$. **(e)** Filtering the residual bunched FFT peak. **(f)** Returning to *real space* pajama of the dissociated ('unbunched') elementary QPs, $\Delta\Phi\cong3\Phi_0$.

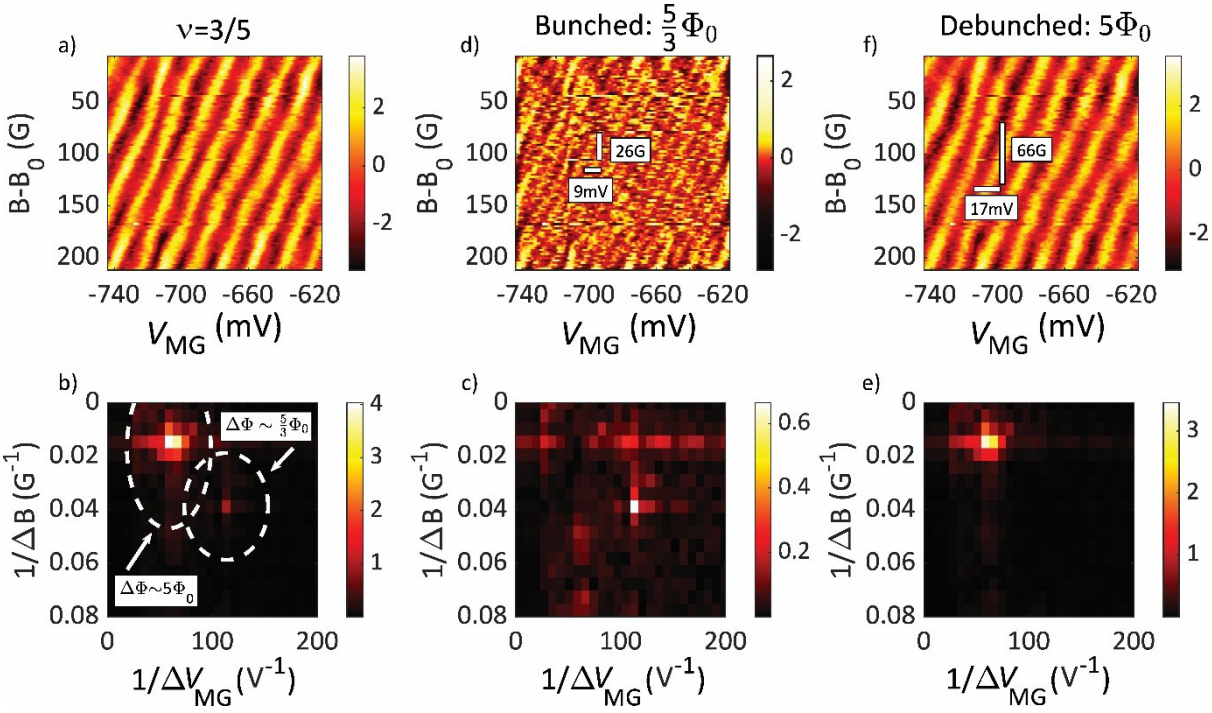

Figure S5b. Separate views of flux periodicities at filling ν=3/5 with charged top gate. (a) A strong peak at $\Delta\Phi\cong 5\Phi_0$ (dissociated QPs) and a residual peak at $\Delta\Phi\cong(5/3)\Phi_0$ (bunched QPs) **(b)** Two corresponding peaks in the FFT. The dotted ovals indicate the radius of the Gaussian filtering applied later. **(c)** Removing the dissociated FFT peak at $5\Phi_0$ by Gaussian filtering and leaving the weaker peak of the bunched QPs. **(d)** Returning to *real space* pajama of the bunched QPs, with periodicity $\Delta\Phi\cong(5/3)\Phi_0$. **(e)** Filtering the residual bunched FFT peak. **(f)** Returning to *real space* pajama of the dissociated elementary QPs, $\Delta\Phi\cong 5\Phi_0$.

S6. The effect of temperature on the interference

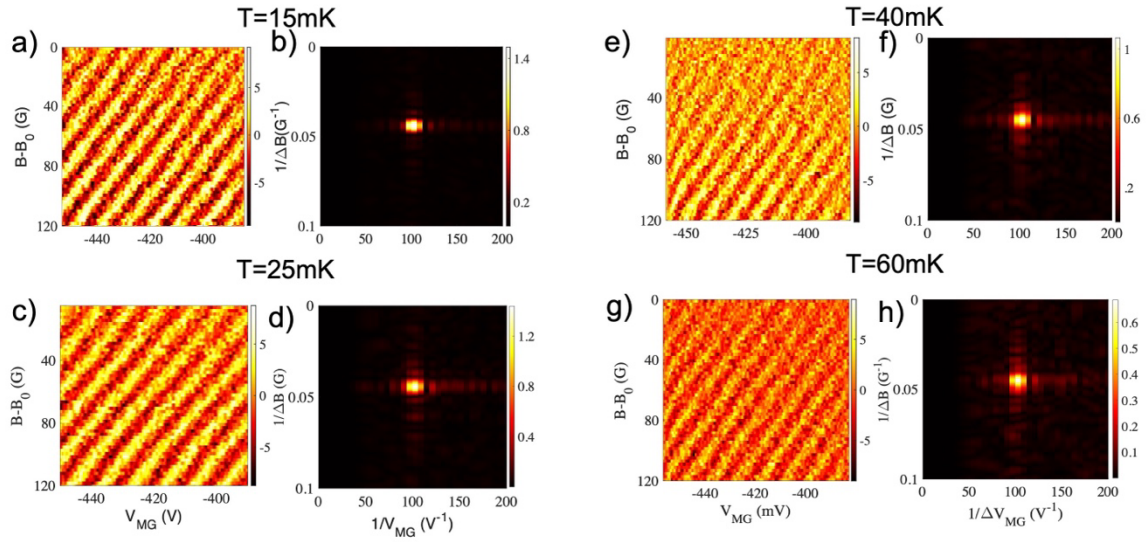

Figure S6. **The effect of temperature increase on the bunching of QPs at ν_b=3/5.** AB interference at an elevated electron temperature in the range 15-100mK with QPCs transmission of: $T_1 = T_2$=0.8. In the range 15-60mK the visibility remains nearly constant (~1%) while the 2D-FFT plots remain with a single prominent peak of bunched QPs, $\Delta\Phi \sim (5/3)\Phi_0$. Above 60mK the visibility drops abruptly. Similar measurements were also performed at ν=2/3 (not shown in the figure), showing qualitatively similar results. The decrease of the visibility with increased temperature prevents an observation of the dissociation.

S7. Bunching and dissociation of the interference in the device with smaller top-gate

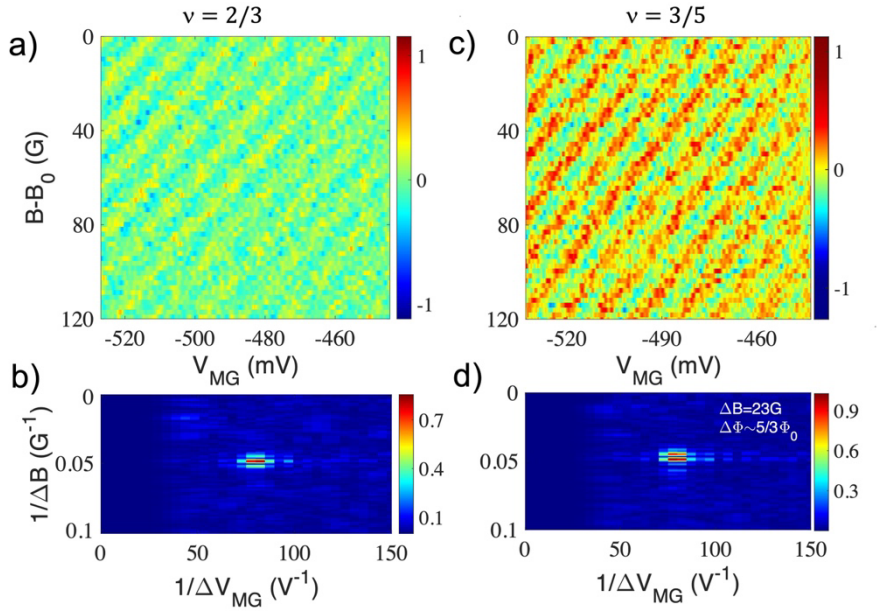

Figure S7a. Aharonov Bohm interference at ν_b=2/3 and 3/5 – Bunching. The OMZI was fabricated on the same wafer. The interferometer area (~3μm^2) and path length (~3μm) similar to the main device described in the text. However, the QPCs are relatively open, and the top-gate area is half of the original one. Here, V_{TG}=0V, with interference of bunched QPs in ν_b=2/3 **(a,b)** and ν_b=3/5 (**c,d**) . The *B*-V_{MG} interference similar to the main device.

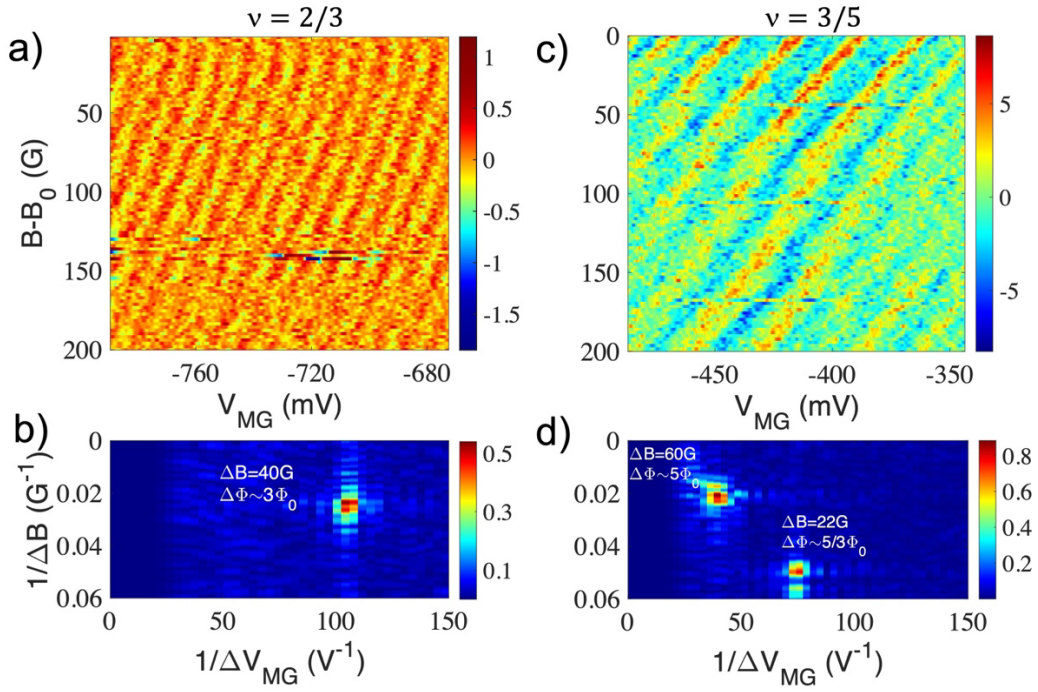

Figure S7b. Aharonov Bohm interference at ν_b=2/3 and 3/5 – Dissociation. Aharonov Bohm oscillation at $\nu_b = 2/3$ and 3/5 for the filling factor configurations **(a)** '1-2/3-0' **(c)** '1-3/5-0'. For this measurement, the top-gate was charged at V_{TG}=+(0.03-0.05)V and the QPCs were tuned to transmission of 90%. 2D FFT shows magnetic flux periodicty corresponding to $\Delta\Phi \cong 3\Phi_0$ for $\nu_b = 2/3$ in **(b)** and $\Delta\Phi \cong 5\Phi_0$ for $\nu_b = 3/5$ in **(d)** suggesting a dissociation of the QPs. Additionally, a small residual harmonic, $\Delta\Phi \cong (5/3)\Phi_0$, indicative of bunched QPs, is present at ν_b=3/5. **(d).** However, this harmonic is absent for $\nu_b = 2/3$ **(b)** (likely due to its low visibility).